PERIÓDICO TCHÊ QUÍMICA
ARTIGO ORIGINAL

ESTUDOS EXPERIMENTAIS DE TRANSFERÊNCIA DE CALOR E MASSA DE MODELOS DE PONTAS PRODUZIDOS A PARTIR DE MATERIAL COMPÓSITO DE CARBONO-CARBONO (MCCC) SOB CONDIÇÕES DE CARGA DE CALOR DE ALTA INTENSIDADE

EXPERIMENTAL STUDIES OF HEAT AND MASS TRANSFER FROM TIP MODELS MADE OF CARBON-CARBON COMPOSITE MATERIAL (CCCM) UNDER CONDITIONS OF HIGH-INTENSITY THERMAL LOAD

ЭКСПЕРИМЕНТАЛЬНЫЕ ИССЛЕДОВАНИЯ ТЕПЛОМАССОПЕРЕНОСА С МОДЕЛЕЙ НАКОНЕЧНИКОВ, ИЗГОТОВЛЕННЫХ ИЗ УГЛЕРОД-УГЛЕРОДНОГО КОМПОЗИЦИОННОГО МАТЕРИАЛА (УУКМ) В УСЛОВИЯХ ВЫСОКОИНТЕНСИВНОГО ТЕРМОСИЛОВОГО НАГРУЖЕНИЯ

SHA, Minggong[1*]; UTKIN, Yuri A.[2]; TUSHAVINA, Olga V.[3]; PRONINA, Polina F.[4];

[1] Northwestern Polytechnical University (NPU), School of Civil Aviation, 127 West Youyi Road, Beilin District, zip code 710072, Xi'an Shaanxi – People's Republic of China.

[2] Moscow Aviation Institute (National Research University), Department of Perspective Materials and Technologies, 4 Volokolamskoe Highway, zip code 125993, Moscow – Russian Federation.

[3,4] Moscow Aviation Institute (National Research University), Institute of Aerospace, Department of Managing Exploitation of Space-Rocket Systems, 4 Volokolamskoe Highway, zip code 125993, Moscow – Russian Federation.

** Correspondence author*
e-mail: 695792773@qq.com

Received 20 April 2020; received in revised form 26 June 2020; accepted 02 July 2020

RESUMO

Os materiais compósitos de carbono-carbono são caracterizados por alta resistência ao calor e estabilidade térmica, para as quais, devido a maioria de suas características físicas e mecânicas, podem ser atribuídos aos materiais mais promissores. Aproximadamente 81% de todos os materiais compósitos de carbono-carbono são utilizados na fabricação de discos de freio para aeronaves, 18% - na tecnologia de foguetes espaciais e apenas 1% - para todas as outras áreas de aplicação. Embora a necessidade de materiais compósitos para tecnologia de foguetes espaciais esteja constantemente diminuindo – o volume de produção de discos de freio para aeronaves está em constante crescimento e, portanto, estudos de propriedades dos materiais compósitos de carbono-carbono sob condições de carga térmica de alta intensidade são extremamente urgentes hoje em dia. Este artigo considera o método para a introdução de silicatos e óxidos nos MCCC, que os endurecem, com a adição de elementos químicos resistentes ao calor. Testes de pontas do MCCC foram realizados sob condições de carga de calor de alta intensidade. Os objetivos do experimento foram obter as formas queimadas do modelo de ponta e registrar a temperatura na superfície durante a ação de um jato que sai do bico do sistema de propulsão. A ponta do MCCC é soprada por meio do sistema de propulsão com um fluxo supersônico de gás contendo oxigênio de alta entalpia. Os resultados de estudos experimentais foram determinados usando gravação de vídeo com base em qual as sequências de quadros foram obtidas. De acordo com os quadros mencionados as formas queimadas foram construídas. Usando medições de imagem térmica, o campo de temperatura na superfície do modelo foi determinado durante todo o tempo em que a superfície do modelo foi exposta ao fluxo de gás supersônico.

Palavras-chave: *material compósito de carbono-carbono, revestimento com proteção térmica, motor de foguete de propulsão líquida, modelo de ponta, características físicas e mecânicas.*

ABSTRACT

Carbon-carbon composite materials are characterized by high heat resistance and thermostability for which they, in most of their physical and mechanical characteristics, can be attributed to the most promising

DOI: 10.52571/PTQ.v17.n35.2020.81_SHA_pgs_988_997.pdf

materials. Approximately 81% of all carbon-carbon composite materials are used for the manufacture of brake rotors for aircraft, 18% – in space rocket technology, and only 1% – for all other areas of application. While the need for composites for rocket and space technology is constantly decreasing – the volume of production of brake disc rotors for aircraft is steadily growing, and therefore research on the properties of carbon-carbon composite materials (CCCM) under conditions of high-intensity thermal loading is extremely urgent at the moment. In this paper, we consider a method for introducing silicates and oxides hardening them with the addition of refractory, chemical elements into CCCM. Tests of tips from CCCM were carried out under conditions of high-intensity thermo-force loading. The objectives of the experiment were to obtain scalded forms of the tip model and to record the temperature on the surface during the action of a jet flowing out of the nozzle of the propulsion system (PS). The tip of the CCCM is blown by means of a propulsion system with a supersonic flow of a highly enthalpy oxygen-containing gas. The results of experimental studies were determined using video recording on the basis of which sequences of frames were obtained on the basis of which the burning forms were built. Using thermal imaging measurements, the temperature field on the model surface was determined during the entire time the supersonic gas flow was exposed to it.

Keywords: *carbon-carbon structural material, thermal insulation coating, liquid rocket engine, tip model, physicomechanical characteristics.*

АННОТАЦИЯ

Углерод-углеродные композиционные материалы характеризуются высокой жаропрочностью и термостойкостью, за что их, по большинству своих физико-механических характеристик, можно отнести к наиболее перспективным материалам. Примерно 81% всех углерод-углеродных композиционных материалов используется для производства тормозных дисков для самолетов, 18% – в ракетно-космической технике и только 1% – для всех остальных сфер применения. В то время как потребность в композитах для ракетно-космической техники постоянно снижается – объем производства тормозных дисков для самолетов стабильно растет, в связи с чем исследования свойств УУКМ в условиях высокоинтенсивного термосилового нагружения на сегодняшний момент крайне актуальны. В данной работе рассматривается метод введения в УУКМ упрочняющих их силицидов и оксидов с добавлением тугоплавких химических элементов. Проведены испытания наконечников из (УУКМ) в условиях высокоинтенсивного термосилового нагружения. Целями эксперимента являлось получение обгарных форм модели наконечника и регистрация температуры на поверхности в процессе воздействия на неё струи, истекающей из сопла двигательной установки (ДУ). Наконечник из УУКМ обдувается при помощи двигательной установки сверхзвуковым потоком высокоэнтальпийного кислородосодержащего газа. Результаты экспериментальных исследований определялись с помощью видеорегистрации на основе которой были получены последовательности кадров, на базе которых были построены обгарные формы. С помощью термовизионных измерений определялось поле температур на поверхности модели в течение всего времени воздействия на неё сверхзвукового потока газа.

Ключевые слова: *углерод-углеродный конструкционный материал, теплозащитное покрытие, жидкостной ракетный двигатель, модель наконечника, физико-механические характеристики.*

1. INTRODUCTION

Carbon-carbon composite materials for most of their physical and mechanical characteristics (FMC) can be attributed to the most promising materials. CCCM are characterized by high heat resistance and thermostability. With intense aerodynamic heating of the thermal protection of hypersonic aircraft, the properties of FMC can change (Bulychev and Kuznetsova, 2019; Ryapukhin *et al.*, 2019; Kozorez and Kruzhkov, 2019; Shen *et al.*, 2019). This is due to the processes of the dynamic interaction of a high-temperature gas flow with the surface of the material. Composite materials of the carbon-carbon system were first created in the early 1960s, simultaneously with the advent of high-strength carbon fibers (Anikin *et al.*, 2019). Obtaining CCCM is based on the principle of heating organic fibers under certain conditions, not destroying them, but turning them into carbon fibers (Kolesnikov *et al.*, 2017; Reznik *et al.*, 2017; Stepashkin *et al*., 2018). Almost all industrial fibers, as well as a number of specially prepared fibers, were tested as feedstock for these purposes. However, most of them did not meet the requirements, the main of which were the non-meltability or ease of imparting it, the yield of the finished fiber, and its high performance. At the same time CCCM contain a carbon reinforcing element in the form of discrete fibers, continuous filaments, and bundles, as well as various

volumetric frame structures (Song, 2009; Babaytsev *et al.*, 2017; Akhmetzhanov *et al.*, 2018; Yin *et al.*, 2018; Evdokimenkov *et al.*, 2019a; Evdokimenkov *et al.*, 2019b; Formalev *et al.*, 2019; Stepashkin *et al.*, 2019).

The advantage of CCCM is that it is able to perceive various external loads due to the fact that the carbon matrix combines the reinforcing elements in a composite (Mohammed *et al.*, 2019). The properties of CCCM vary over a wide range, and its strength characteristics are especially important (Skvortsov *et al.,* 2014; Orlov *et al.,* 2003). To increase the strength of the composite, carbonization of its polymer matrix is carried out by high-temperature heat treatment in a non-oxidizing medium, and then its graphitization is carried out. It is known that the strength of CCCM based on high-strength carbon fibers is higher than the strength of a composite material based on high-modulus carbon fibers obtained at various processing temperatures. Some CCCM, especially those obtained by carbonizing carbon fiber based on organic polymers, are characterized by an increase in strength with an increase in operating temperature up to 2700 ºC. At temperatures above 3000ºC, CCCM are efficient for a short time, since intense graphite sublimation begins (Kabanov *et al.,* 2019; Kolotyrin *et al.,* 2019; Radyuk *et al.,* 2019).

Physico-mechanical characteristics of carbon-carbon composite materials are significantly reduced in oxygen-containing environments when exposed to relatively low temperatures (Doretti *et al.*, 2017; Volovik *et al.,* 2018; Piat *et al.*, 2019). Among the special properties of CCCM are low porosity, low coefficient of thermal expansion, maintaining a stable structure and properties, as well as product dimensions. Here, we consider the development of a method for introducing silicides and oxides hardening them with the addition of refractory, chemical elements into the CCCM, which allows us to ensure the functioning of the fired forms of the tip models and to record the temperature on the surface in the process of exposure to a high-enthalpy stream of the oxygen-containing gas.

The mechanical strength of solids is determined by the strength of the interatomic bond. Of the natural bodies, diamond has the highest hardness, in which there are carbon-carbon interatomic bonds. Carbon-carbon bonds are also present in graphite; it has a layered structure. There are strong carbon-carbon bonds inside the layers. These bonds are used to create high strength materials. One of the important problems of creating designs of aviation, aircraft and rocket engines is the development of new materials used for the manufacture of the most loaded parts operating under high temperatures (Djugum and Sharp, 2017; Wu and Yan, 2018; Wang and Zhu, 2018; Xie *et al.*, 2019).

Carbon-carbon composite materials – a new class of structural materials designed to create heat-loaded, durable, tough products operating in aggressive environments (Chen *et al*., 2018; Zhang *et al.*, 2019). Products from similar materials are used to create parts for aircraft, rocket devices, and engines. They have a unique ability to maintain high strength and stiffness at temperatures up to 2700 ºC, and coating provides performance in an oxidizing environment. Multidimensionally reinforced CCCM are materials based on a carbon matrix and a woven frame of three- or four-dimensional carbon fiber structures. Designed for use in rocketry products operating at high temperatures. It is produced in the form of cylindrical billets and parallelepipeds using serial technologies. Antioxidant coatings are applied to parts operating under high-enthalpy flow products (Mei *et al.*, 2017; Wang *et al.*, 2019). These coatings consist of adhesive and erosion resistant antioxidative layers. The adhesive layer is made on the basis of tantalum carbide, which provides high mechanical bond strength of the erosion-resistant antioxidant coating with CCCM. The main method for testing products is to create conditions as close as possible to the conditions in which the product will work. This is gas-dynamic heat load, creation of an oxidizing environment, vacuum (Davydovich *et al*., 2017).

2. MATERIALS AND METHODS

A tip model made of the composite material was manufactured for the experiment. An antioxidant coating was applied to the tip. Material characteristics are as follows:

– density, 1.67 g / cm^3;

– porosity 2.5%;

– thermal conductivity 2.6 W / m;

– ultimate tensile stress at 260 MPa;

– tensile modulus 75 MPa;

– breaking stress at compression 140 MPa;

– Poisson's ratio 0.12.

To create a high-temperature free flow from the engine nozzle to the tip on the stand, a liquid rocket engine operating on liquefied oxygen-hydrogen gas is used. The engine using oxygen-

hydrogen fuel in specific impulse is approximately 30% higher than oxygen-kerosene.

The engine consists of a mixing head with pressure jet atomizers, a combustion chamber, and a nozzle. The engine uses a Laval nozzle. It represents a gas channel of a special profile having a narrowing to change the speed of the gas stream passing through it. It is an important part of modern rocket engines. For a video recording of experiments, two video cameras were used, with a recording rate of 30 frames per second, network cable, two opto-digital converters, neutral light filters.

Temperature measurements were made with a thermal imager. Thermal radiation from the surface of the cone passes through the filters and through the lenses of the lens, which forms the image of the cone on the camera matrix. Each matrix element forms a signal proportional to the perceived radiation energy. This signal is digitized and transmitted to the computer via the USB port. On a computer using software, the data is processed, and the thermal radiation of the object is visualized in real-time. Video recording was carried out with a shot breakdown of 30 frames per second, which allowed the construction of combusted forms.

The start of thermal registration was carried out before the start of the experiment. A thermogram was shown on the computer with the maximum tip temperature recorded during the experiment. Thermal registration allowed us to determine the maximum surface temperatures achieved during the experiments. The pressure in the chamber and at the nozzle exit was registered by sensors.

Additional methods using plasmatrons and other equipment were not used.

3. RESULTS AND DISCUSSION:

The schematic diagram of the video and thermovisual fixation of the experiment is shown in Figure 1, which shows the overtaking flow coming out from the nozzle of a propulsion system (PS) (1), the investigated model of CCCM (2), a quartz optical window (3), a VideoScan-415 camera (4), a Nikon NIKKOR-52AF lens (5), a filter package consisting of a cut-off filter LP850 and a neutral filter ND8 (6), moreover, objects 4, 5 and 6 together constitute the Tandem VS-415-V2 thermal imager, camera-controller connection 5 m long (7), a laptop with the TERMO-6 thermal imager software installed and data recorded (8), a network cable ~ 60 m long connecting the recording and controlling laptops (9) located in the control room at a distance of ~ 50 m from the laptop from which control of a laptop connected to a thermal imager is carried out, including data logging control (10).

The video recording complex consists of a laptop, from which data of video cameras are recorded, a network cable-twisted pair (12), with which the laptop was connected to a fiber optic path, which consisted of analog-to-digital converters (13) and fiber itself (14). The cameras (16, 17) were connected to an analog-to-digital converter using network cables-twisted pairs (15). The distance from the cameras and the thermal imager to the model was ~ 4 m. Both devices were located in a separate room next to the stand on an isolated foundation, which allowed to reduce the level of equipment vibration.

Tip models were tested on a bench stand. The bench setup included: an oxygen-hydrogen chamber with a critical section diameter of 92 mm, a holder, an ignition unit, and spark plugs. The model was attached to the stand holder through a spacer. The spacer on the outside was covered with a fairing. The distance of the model from the nozzle exit before testing was 40 ± 0.5 mm.

The duration of the propulsion system in a given mode was 10 s. Samples were measured after testing. The propulsion system worked at the set modes, the temperature at the cut of the chamber was 2780°C, the discharge velocity was 1742 m/s. The objective of the experiment was to obtain scalded forms of the tip model and to register the temperature at the surface during the action of a jet flowing from the remote-controlled nozzle. To achieve these goals, thermal imaging measurements and video recording of the experiment process were carried out as part of the CCCM test program.

The purpose of the video recording is to obtain a sequence of frames on the basis of which the burning forms are built. Using thermal imaging measurements, the temperature field was determined on the model surface during the entire time the jet was exposed to it. The models were a cone with spherical blunting. The half-angle of the cone solution was 7°, and the radius of the spherical blunting was 36 mm. The total length of the model was 125 mm. It should be noted that the models consisted of three parts: the tip of the CCCM material, the stern, and the conical insert along the central axis.

For a video recording of experiments, two video cameras were used. One recorded the general view of the stand during the tests (SONY),

and the second fixed the sample from the angle as close as possible to the thermal imager (JAI), which is designed for non-contact measurement of the temperature of the studied objects. The thermal imager was connected via a communication cable to a PC with the installed VS2001 controller, on which the TERMO 6 software was installed, and on which the obtained thermal images were recorded. PC data management was carried out remotely from the stand control center (Krayushkina *et al.,* 2019).

Thermal radiation from the surface of the object under study passed through the filters and through the lenses of the camera, which forms the image of the object on the CCD matrix of the camera. Each element of the CCD matrix forms a signal proportional to the perceived radiation energy. This signal is digitized and transmitted to the computer via a USB port. On a computer using the TERMO 6 software, the obtained data is processed, and the thermal radiation of the object is visualized in real-time, as well as the reproduction of single thermal images and sequences of thermal images in video mode, as well as a retrospective analysis of the obtained data. It must be clarified that after processing the signal of the TERMO 6 software, a thermogram is formed with temperatures corresponding to the brightness temperature adjusted for the degree of blackness of the test sample (Yuilin *et al.,* 2019).

Further, the term “true temperature” will be used for this temperature. In this case, the actual temperature of objects in some cases may differ from the true temperature recorded by the thermal imager. The video recording was launched by the clock signal received directly from the stand with the following parameters:

- registration speed ~ 6 frames per second;

- degree of blackness – 0.9;

– ambient temperature – 17ºC;

– λ is the specified coefficient of the medium transmittance (quartz window) – 0.93;

– distance to the sample – 4 m.

The start of thermal registration was carried out manually, before starting. Figure 2 shows a sample before starting. The initial shape of the sample and its position relative to the nozzle are clearly visible. Figure 3 shows a thermogram with temperature decoding. The temperature profile in the “Profile XY” window (3) is calculated along the horizontal line visible on the thermogram (1). In the rectangular region (2), the maximum temperature, the average value, and the number of parameters are calculated. The recorded true temperature of the gas in the shock layer (6) reaches 1900 ºC. In region (6), a jet is seen flowing out of the propulsion system nozzle.

During the experiment, video recording and thermal recording were carried out, which allowed us to construct the diagrams shown in Figure 4 and build the charred forms. Here is a diagram of the distribution of the temperature field (Ta) and the flow velocity at the nozzle exit (Wa) at different points in time. Figures 5-6 show the appearance of the tip model before and after the test.

As a result of the high-intensity effect of gas-dynamic and thermal loads, the material was carried away from the tip. The ablation of the material largely depends on the heat resistance, heat resistance, and mechanical strength of the tips, which largely depends on the weaving of the fabric, the number of layers of their orientation, epoxy fillers, hardening of products by coating tantalum carbide, silicon. All of the above properties affect the physical and mechanical characteristics. Thanks to video cameras, frames were sequentially obtained on the basis of which rainfed forms were built. Thermal imagers measured the temperature fields on the surface of the tips during the entire time the jet was exposed to them. Tips made of aluminum alloys, stainless steel, titanium could not withstand such loads when conducting similar experiments.

4. CONCLUSIONS:

Therefore, on the basis of the experimental studies carried out in the work, the following data is obtained: experimental dependences of the burning forms of the models on time, data on the distribution of temperature and velocity of the jet outflow on the surface of the models. A diagram of the distribution of the temperature field and the flow velocity as a function of time is shown, from which it can be seen that the jumps in the temperature field are synchronized with the jumps of the velocity vector at times of 3.5 and 5 min. It also illustrated the process of ablation of the mass of the tip when exposed to high-speed high-enthalpy gas flow.

It can be seen from the experimental work that the CCCM retains high heat resistance and heat resistance at high gas-dynamic loads and high temperatures. Experiments have shown that CCCM accepts temperature and gas-dynamic loads due to the fact that the carbon matrix combines the reinforcing elements in CCCM. To increase the strength of CCCM, carbonization of its matrix was carried out, due to which the heat

resistance, heat resistance, erosion resistance of the products were significantly increased.

5. ACKNOWLEDGMENTS:

The work was carried out with the financial support of the state project of the Ministry of Education and Science project code “Modern technologies of experimental and digital modeling and optimization of spacecraft systems parameters”, project code FSFF-2020-0016

6. REFERENCES:

1. Akhmetzhanov, R.V., Balashov, V.V., Bogachev, Y.A., Yelakov, A.B., Kashirin, D.A., Svotina, V.V., Spivak, O.O., *and* Cherkasova, M.V. (2018). An ion thruster accelerating electrode made of carbon-carbon composite material. *Thermal Engineering*, *65*(13), 986-993.
2. Anikin, A.V., Berdov, R. D., Volkov, N.N., Volkova, L.I., Gurina, I.N., *and* Tsatsuev, S.M. (2019). Long-run testing of model nozzle extensions made of a carbon-carbon composite material in a liquid-propellant rocket engine operating on hydrogen and oxygen. *Journal of Applied Mechanics and Technical Physics*, *60*(1), 80-86.
3. Babaytsev, A.V., Prokofiev, M.V., *and* Rabinskiy, L.N. (2017). Mechanical properties and microstructure of stainless steel manufactured by selective laser sintering. International *Journal of Nanomechanics Science and Technology*, *8*(4), 359-366.
4. Bulychev, N.A., *and* Kuznetsova, E.L. (2019). Ultrasonic Application of Nanostructured Coatings on Metals. *Russian Engineering Research*, *39*(9), 80-812.
5. Chen, B., Wen, W., Cui, H., Zhang, H., *and* Xu, Y. (2018). Test on mechanics of three-dimensional four directional C/C composites at elevated temperature and oxidation environment. *Hangkong Dongli Xuebao/Journal of Aerospace Power*, *33*(8), 1916-1922.
6. Davydovich, D., Dron, M., Zharikov, K., *and* Iordan, Y. (2017). Research of the launch vehicle design made of composite materials under the aerodynamic, thermal and acoustic loadings. *MATEC Web of Conferences*, *102*, article number 01011.
7. Djugum, R., *and* Sharp, K. (2017). The fabrication and performance of C/C composites impregnated with TaC filler. *Carbon*, *115*, 105-115.
8. Doretti, L., Longo, G.A., Mancin, S., Righetti, G., *and* Zilio, C. (2017). Flow boiling heat transfer on a Carbon/Carbon surface. *International Journal of Heat and Mass Transfer*, *109*, 938-948.
9. Evdokimenkov, V.N., Kim, N.V., Kozorez, D.A., *and* Mokrova, M.I. (2019a). Control of unmanned aerial vehicles during fire situation monitoring. *INCAS Bulletin*, *11*, 67-73.
10. Evdokimenkov, V.N., Kozorez, D.A., *and* Krasilshchikov, M.N. (2019b). Development of pre-flight planning algorithms for the functional-program prototype of a distributed intellectual control system of unmanned flying vehicle groups. *INCAS Bulletin*, *11*, 75-88.
11. Formalev, V.F., Kolesnik, S.A., *and* Kuznetsova, E.L. (2019). Effect of components of the thermal conductivity tensor of heat-protection material on the value of heat fluxes from the gasdynamic boundary layer. *High Temperature*, *57*(1), 58-62.
12. Kabanov, E.I., Korshunov, G.I., *and* Gridina, E.B. (2019). Algorithmic provisions for data processing under spatial analysis of risk of accidents at hazardous production facilities. *Naukovyi Visnyk Natsionalnoho Hirnychoho Universytetu, 2019*(6): 117-121.
13. Kolesnikov, S.A., Kim, L.V., Vorontsov, V.A., Protsenko, A.K., *and* Cheblakova, E.G. (2017). Study of thermophysical property formation of spatially reinforced carbon-carbon composite materials. *Refractories and Industrial Ceramics*, *58*(4), 439-449.
14. Kolotyrin, K.P., Bogatyrev, S.A., Savon, D.Y., *and* Aleksakhin, A.V. (2019). Use of resource-saving technologies in fabrication and restoration of steel bushing-type components via hot plastic deformation. *CIS Iron and Steel Review, 18*, 38-41.
15. Kozorez, D.A., *and* Kruzhkov, D.M. (2019). Autonomous navigation of the space debris collector. *INCAS Bulletin*, *11*, 89-104.
16. Krayushkina, K., Khymeryk, T., *and* Bieliatynskyi, A. (2019). Basalt fiber concrete as a new construction material for roads and airfields. *IOP Conference Series: Materials Science and Engineering, 708*, Article number 012088.
17. Mei, X., Zhang, X., Liu, X., *and* Wang, Y. (2017). Effect on structure and mechanical property of tungsten irradiated by high-

intensity pulsed ion beam. *Nuclear Instruments and Methods in Physics Research, Section B: Beam Interactions with Materials and Atoms*, *406*, 697-402.

18. Mohammed, A.S.K., Sehitoglu, H., *and* Rateick, R. (2019). Interface graphitization of carbon-carbon composites by nanoindentation. *Carbon*, *150*, 425-435.
19. Orlov, A.M., Skvortsov, A.A., *and* Litvinenko, O.V. (2003). Bending vibrations of semiconductor wafers with local heat sources. *Technical Physics, 48*(6): 736-741.
20. Piat, R., Zuo, Y., *and* Megyesi, P. (2019). Numerical modeling of the 2D crack propagation in carbon-carbon composites. *Ceramic Engineering and Science Proceedings*, *39*(3), 89-104.
21. Radyuk, A.G., Gorbatyuk, S.M., Tarasov, Y.S., Titlyanov, A.E., Aleksakhin, A.V. (2019). Improvements to mixing of natural gas and hot-air blast in the air tuyeres of blast furnaces with thermal insulation of the blast duct. *Metallurgist, 63*(5-6), 433-440.
22. Reznik, S.V., Mikhailovskii, K.V., *and* Prosuntsov, P.V. (2017). Heat and mass transfer in the chemical vapor deposition of silicon carbide in a porous carbon–carbon composite material for a heat shield. *Journal of Engineering Physics and Thermophysics*, *90*(2), 291-300.
23. Ryapukhin, A.V., Kabakov, V.V., *and* Zaripov, R.N. (2019). Risk management of multimodular multi-agent system for creating science-intensive high-tech products. *Espacios*, *40*(34), 19-32.
24. Shen, Q., Song, Q., Li, H., Xiao, C., Wang, T., Lin, H., *and* Li, W. (2019). Fatigue strengthening of carbon/carbon composites modified with carbon nanotubes and silicon carbide nanowires. *International Journal of Fatigue*, *124*, 411-421.
25. Skvortsov, A.A., Kalenkov, S.G., *and* Koryachko, M.V. (2014). Phase transformations in metallization systems under conditions of nonstationary thermal action. *Technical Physics Letters*, *40*(9), 787-790.
26. Song, M. (2009). Effects of volume fraction of SiC particles on mechanical properties of SiC/Al composites. *Transactions of Nonferrous Metals Society of China*, *19*(6), 1400-1404.
27. Stepashkin, A.A., Ozherelkov, D.Y., Sazonov, Y.B., *and* Komissarov, A.A. (2018). Criteria for evaluating the fracture toughness of carbon–carbon composite materials. *Metal Science and Heat Treatment*, *60*(3-4), 266-272.
28. Stepashkin, A.A., Ozherelkov, D.Y., Sazonov, Y.B., Komissarov, A.A., *and* Mozalev, V.V. (2019). Change in interlayer strength and fracture toughness of carbon-carbon composite material under the impact of cyclic loads. *Inorganic Materials: Applied Research*, *10*(1), 155-161.
29. Volovik, A.Y., Krylik, L.V., Kobylyanska, I.M., Kotyra, A., *and* Amirgaliyeva, S. (2018). Methods of stochastic diagnostic type observers. *Proceedings of SPIE – The International Society for Optical Engineering*, *10808,* Article number 108082X.
30. Wang, B., Xu, B., *and* Li, H. (2019). Fabrication and properties of carbon/carbon-carbon foam composites. *Textile Research Journal*, *89*(21-22), 4452-4460.
31. Wang, M., *and* Zhu, W. (2018). Pore-scale study of heterogeneous chemical reaction for ablation of carbon fibers using the lattice Boltzmann method. *International Journal of Heat and Mass Transfer*, *126*, 1222-1239.
32. Wu, Q.-J., *and* Yan, H. (2018). Fabrication of carbon nanofibers/A356 nanocomposites by high-intensity ultrasonic processing. *Metallurgical and Materials Transactions A: Physical Metallurgy and Materials Science*, *49*(6), 2363-2372.
33. Xie, W., Yang, Y., Meng, S., Peng, T., Yuan, J., Scarpa, F., Xu, C., *and* Jin, H. (2019). Probabilistic reliability analysis of carbon/carbon composite nozzle cones with uncertain parameters. *Journal of Spacecraft and Rockets*, *56*(6), 1765-1774.
34. Yin, T., Li, X., Wang, Y., He, L., *and* Gong, X. (2018). Effect of the meso-structure on the strain concentration of carbon-carbon composites with drilling hole. *Science and Engineering of Composite Materials*, *25*(4), 825-834.
35. Yuilin, H., Beljatynskij, A., *and* Ishchenko, A. (2019). Non-Roundabout design of cancel the intersection signal light on horizontal plane. *E3S Web of Conferences, 91*, 1-22.
36. Zhang, Q., Zhu, X.P., Zhang, C.C., *and* Lei, M.K. (2019). Comprehensive material constraints incorporation in coupled thermal-mechanical responses modelling for high-

intensity pulsed ion beam processing of metals. *Nuclear Instruments and Methods in Physics Research, Section B: Beam Interactions with Materials and Atoms*, *461*, 283-291.

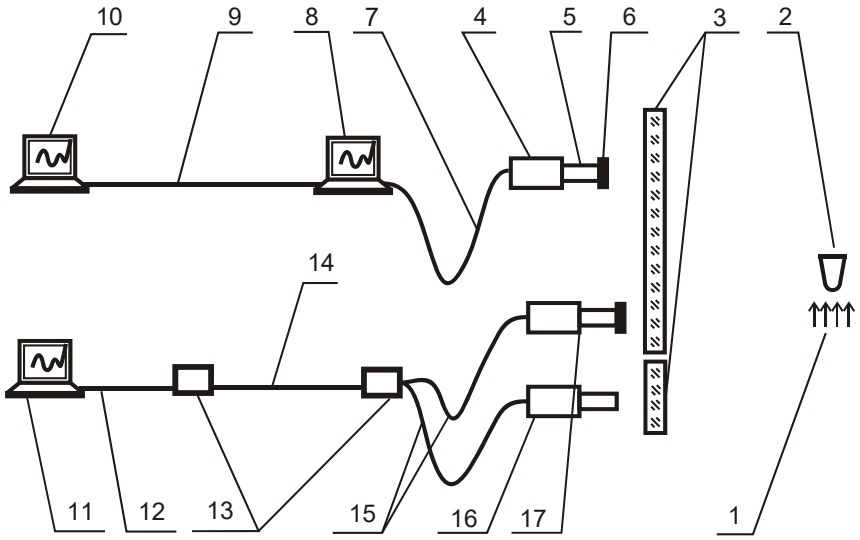

Figure 1. *Schematic diagram of the experiment for measuring the temperature of a sample streamlined by a supersonic jet flowing out of a propulsion system*

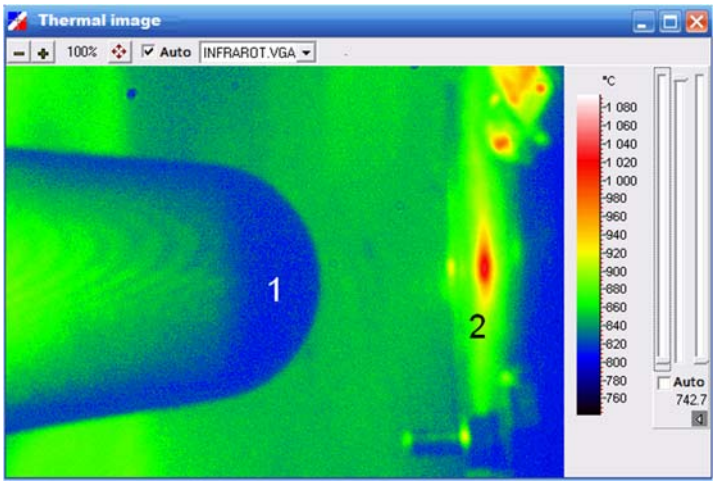

Figure 2. *Sample before starting (1 - sample, 2 – cut-off of propulsion system nozzle)*

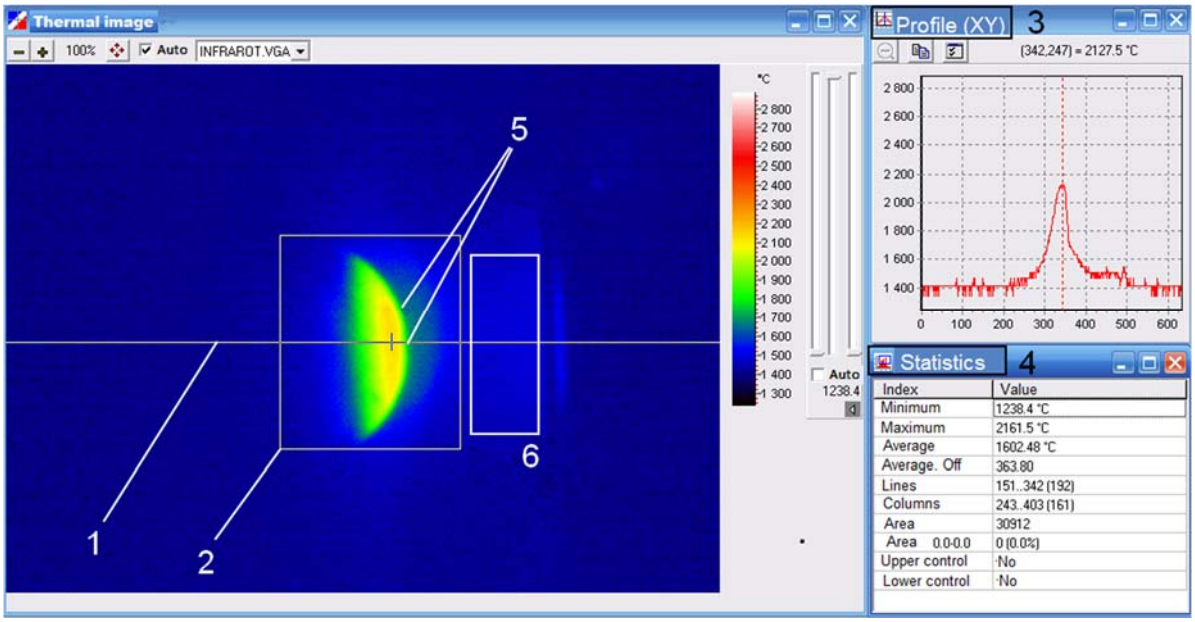

Figure 3. *The first frame after heating of the sample*

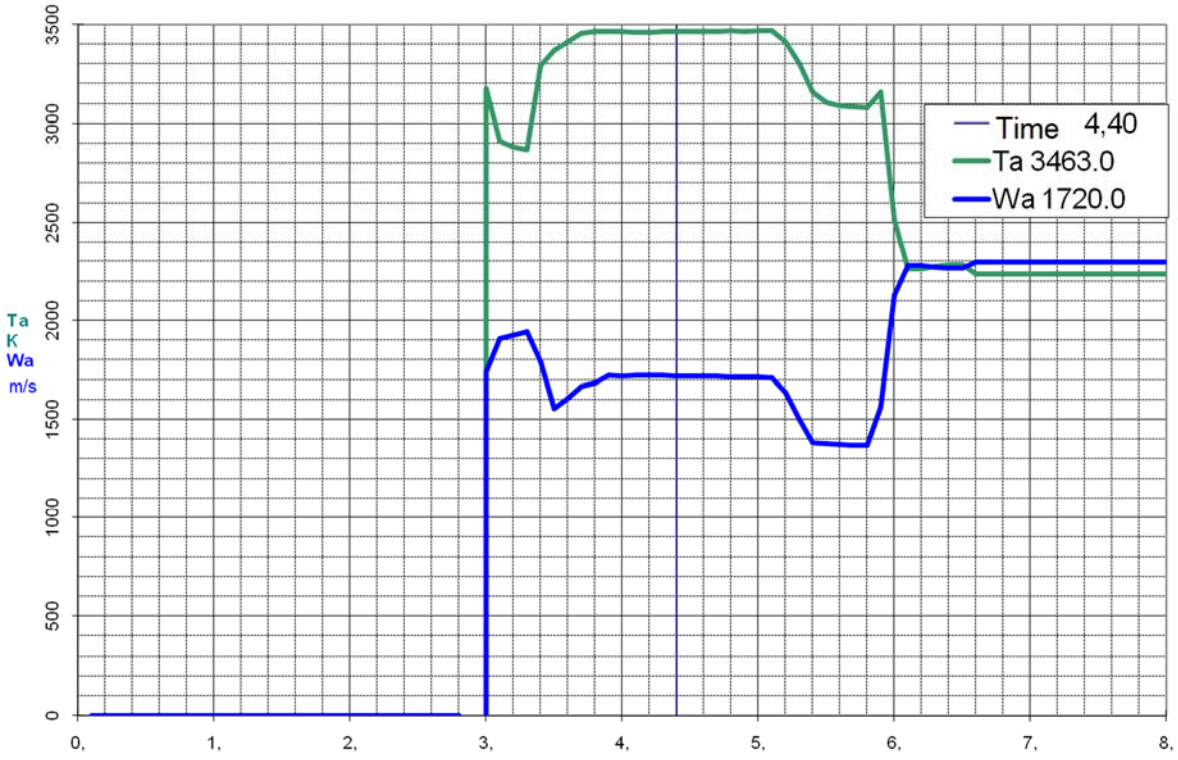

Figure 4. *Diagram of temperature (Ta) and jet velocity (Wa)*

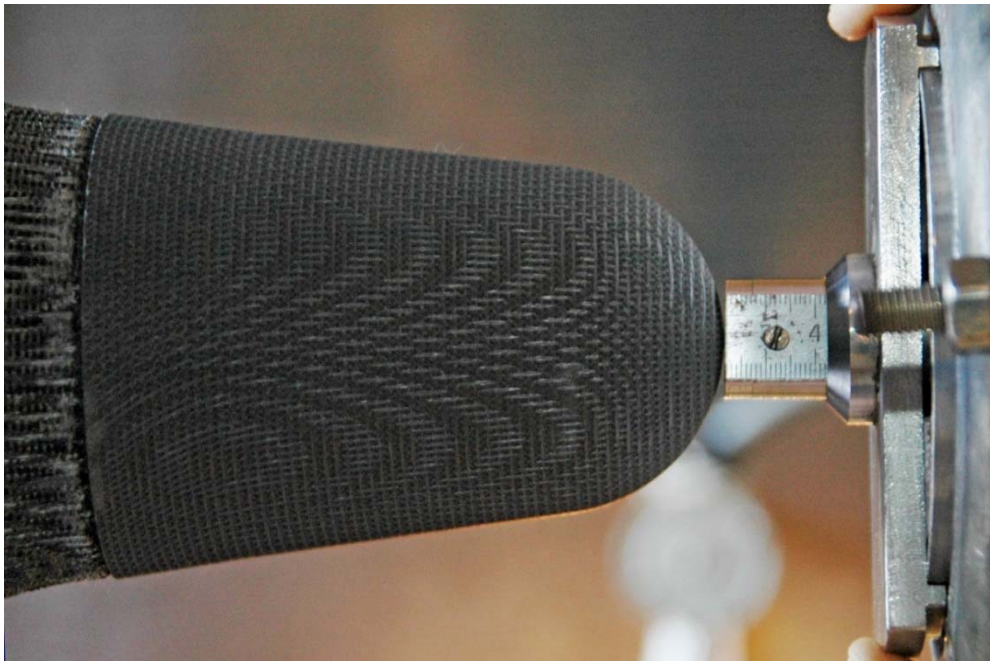

Figure 5. *Tip model view before the test*

Figure 6. *Tip model view after the test*